Mathematical Statistician and Engineering Applications
ISSN: 2094-0343
2326-9865

Numerical Simulation to Evaluate air Pollutants Resulting from Fuel Combustion in a Thermal Power Plant under Different Conditions

Rafid M. Hannun[1] and Ali H. Abdul Razzaq[2]

[1,2] Department of Mechanical Engineering, College of Engineering, University of Thi-Qar, ThiQar, 64001, Iraq.

[1,2] Email: Rafid-m@utq.edu.iq, ali.hussein.a@utq.edu.iq

Article Info

Page Number: 5977 - 5999

Publication Issue:

Vol 71 No. 4 (2022)

Abstract

Predicting the release of pollutant concentrations into the atmosphere is an essential element in assessing potential environmental damage from industrial emissions. This paper presents a numerical study to model the dispersion of pollutants from the stacks of the thermal power plant in Nassiriya, Iraq. The power plant operates on two types of fossil fuels (crude oil and natural gas) and emits pollutants in the form of (CO, CO_2, SO_2, and NO_X). A 3D mathematical model based on fluid mechanics equations is used in conjunction with a modified standard k-ε turbulence model to calculate flow and scattering at the atmospheric microscale (for distances of several kilometers). In order to confirm the current study's validity, the created numerical model was compared with the previous experimental and theoretical models, and the comparison results showed good agreement. These equations were solved using the ANSYS FLUENT (CFD) 2020 R2 program to show the results of flowing smoke columns at variable factors of wind speed, pollutant columns, stack heights, and wind direction angles.

The findings of this investigation demonstrated that the numerical model correctly predicts the column path and its concentrations. The results indicated that the concentration of pollutants in liquid fuels (crude oil) is higher than the concentration of pollutants in gaseous fuels (natural gas), where the maximum concentration of carbon dioxide (CO2) in liquid and gaseous fuels at a wind speed of (2) m/s and a distance of 203 m is (0.0000362, 0.00235), respectively.

Keywords: Reynolds-averaged Navier–Stokes, Thermal power plant, Pollutant dispersion, SIMPLE algorithm.

Article History

Article Received*: 25 March 2022*

Revised*: 30 April 2022*

Accepted*: 15 June 2022*

Publication*: 19 August 2022*

1. Introduction

Reduced air pollution is a critical component of promoting long-term development. One of the global and localized challenges is air pollution, which is primarily caused by energy generation and use. It has consistently contributed to global warming over time. Energy is essential in all aspects of life in today's world. It is critical for industrial production, transportation fuel, and energy generation in thermal power plants. The exponential growth of the world's population is inextricably linked to increased energy consumption and environmental concerns [1]. Using the finite volume method with crude oil and gaseous fuel in the furnace of the Nasiriya power plant, three-dimensional aerodynamic and thermal predictions at investigated liquid fuel combustion (crude oil or mazut) are solved using the discrete phase model to obtain an acceptable temperature distribution, velocity, and other results. The maximum temperature (at the furnace center between the upper and lower burners) is 2293 K, but the Fluent software code found it to be 2299.45 K. In addition, he discovered that when a gaseous fuel was used, the highest temperature reached 2152 K in practice and 2215 K in theory[2]. investigated the retrofitted steam generating furnace in a thermal power plant using numerical models. A precise mathematical furnace model was created with a detailed 3D mesh that includes all critical aerodynamic and thermochemical processes of the furnace. The research focuses on the environmental aspect of the combustion of two fuels, especially on the production of pollutants such as (CO_2, SO_2, SO_3, NOx, and soot) [3]. used a two-dimensional mathematical model based on fluid mechanics equations, using a modified non-isotropic k- ε turbulence model (distances on the order of kilometers). The model is implemented in a two-dimensional computational code that uses body-fitted coordinates and is based on the finite volume approach to analyze flow and dispersion at the atmospheric microscale. The study results are obtained by solving the average Navier-Stokes equations and the turbulent k-ε model using the finite volume method (FVM). The calculations were performed for an exhaust gas flow from an industrial stack with different gas velocities (4, 10, and 14) m/s, wind speeds (2, 4, 8, and 10) m/s, and stack heights (50, 75, and 100) m/s [4]. performed a case study for the Nassiriya power plant with variable loads of units (70- 210) MW_E. The pollutants produced by fuel-burning (liquid or gas) refineries were explored by modeling the released gases in furnace chambers. Using the FLUENT computer code, the finite volume approach was investigated to anticipate pollutant parts. The case study was created graphically and then transferred into FLUENT to be solved. These pollution species are (NO_X and SO_X), major air pollutants that impact human health. The combustion

temperature is higher than when utilizing gaseous fuel. As a result, the maximum (NOx) emissions for gaseous fuel firing are at a load of 70 MW and gradually decrease with increasing load until they reach a minimum value at maximum load (210 MW)[5]. performed a high-resolution simulation numerically of the dispersion of near-and far-field pollutants in a series of buildings in the city centers of Hannover and Frankfurt am Main, using ANSYS FLUENT 17.0, a commercial CFD program, to simulate airflow and pollutant dispersion. For all settings, the species transport model, dynamic Smagorinsky (SGS), and LES are used to simulate the pollutant dispersion. For the investigation, methane and carbon dioxide are employed. The computing domain has the following measurements: L = 500 m in length, W = 500 m in width, and H = 300 m in height. The computational domain also has the following measurements: L = 600 m in length, W = 580 m in width, and H = 200 m in height. An intake velocity of 2.8 m/s, a temperature of 310 K, and an inlet wind speed of 9 m/s are used in the city of Hannover[6]. performed a computational simulation of the dispersion of pollutants produced during the combustion of fuels and their chemical reactions in the atmosphere. The dispersion of (NO_2, CO, NO_2, HNO_3, and CO_2) during a chemical reaction with oxygen was studied in a natural thermal power plant with two stacks of (300, 330) in height and a wind speed of 3 m/s. A primary objective was to determine how pollution can be found at different distances from the point of origin of the pollutant at (1000,1500,2500,3000,10000)m. Three test problems were used to validate the numerical method. Numerous test problems were used to select the best turbulence models (k- ε and k- ω). The pollutants were found not to mix immediately, but active mixing at 500 m from the source showed the mass fraction of the stack at 330 m height to be higher than the stack at 300 m height [7]. used the BREEZE ISC GIS-Pro model to rapidly assess the impact of gaseous emissions on ambient air quality in the region at the Al-Hartha power plant. The station has four stacks, and the stack height is 100 m. The diameter of the upper stack is 403 m (internal), 4.7 m (external), and the diameter of the lower stack is 5.3 m (internal), and 6.5 m (external). The flow rate of exhaust gases is 81400 kg/h. The exit velocity of gases is 15.58 m/s and the exit temperature of gases is 428–433 K. Maximum annual temperatures can reach 47ºC with an average of 25ºC. The prevailing wind is northwest, and wind speeds reach more than 10.8 m/s. They were considering different scenarios to assess the potential exposure and health effects at near distances in the vicinity of the plant (up to 1.5 km, in close range) and long distances up to the Kuwaiti and Iranian borders. Because on-site emission measurements were unavailable, SO2 emission rates were estimated based on fuel quantity and quality[8]. used the LAKES ENVIRONMENTAL program to simulate the effects of air pollution from the Doura

refinery stacks. The presence of these chemicals in the crude oil feedstock resulted in (NOx, SOx, and CO2) emissions from the refinery's combustion processes. The stacks range in height from 10 to 30 m and in diameter from 1 to 3 m. The gas exiting the stack has a diameter of 2.5 m, a velocity of 25 m/s, a temperature of 450 K and an ambient temperature of 29oC. At velocities ranging from 1 m/s to 20 m/s, all categories of atmospheric stability were investigated [9]. This paper aims to find standard solutions to air pollution issues produced by fossil fuel burning in thermal power plants, allowing for the prevention of lethal respiratory diseases. It also critically reviews the increased awareness of the significance of pollution control studies in places where thermal power plants were being built for electricity generation.

2. Thermal Power Station

The power plant is one of the most critical topics studied, and the furnace is an integral part of the boiler, as it is at the beginning of the power generation process and is directly related to the efficiency of the cycle. Industrial furnaces and boilers provide steam or hot water in the manufacturing, processing, mining, and refining industries. The design of flames for furnaces and combustion chambers for industrial purposes is still an art in which the designer applies practical knowledge, as he must analyze in detail the complex physicochemical processes in flames. An ever-increasing number of researchers and designers are attracted by the ever-increasing power of power units, the application of flames in aviation, and the problem of minimizing pollution caused by combustion. Water-tube furnaces vary significantly depending on the designer's perspective, power requirements, fuel source, and burner design. At the Nassiriya power plant (current case study), steam is generated in vertical tubes arranged to form the combustion chamber walls in an internally fired natural circulation drum-type boiler. Steam and water are separated in the boiler drum, and the remainder of the water, together with the incoming feed water, is returned to the water tubes of the combustion chamber through down comers, i.e., piping outside the combustion chamber. The steam exiting the boiler enters the superheated, which is further heated before being fed into the turbine in the furnace. The steam from the turbine can be returned to the plant and reheated in the reheater. Since high-temperature deposits can form in a superheater zone if the gas at the furnace outlet is too hot, the temperature must be sufficiently low to avoid this. However, it must be high enough to allow the superheater, economizer, and air heater design. The influence of finite volume analysis using ANSYS FLUENT on the temperature distribution in this furnace and the other parameters of the gas products in x, y, and z directions for two different fuel types (liquid and gaseous fuel) is also

studied to better understand the performance of the furnace and achieve higher efficiency. Certain variables, such as the average velocity of fuel and air, are estimated using mass flow rates and furnace temperatures, while the pressure is calculated using an empirical equation provided by the power plant's contracting company [2].

3. Problem description

The problem of modeling the effects of the combustion products of the Nassiriya power plant on the ambient air of the city was studied, as shown in Fig. (1). It will be shown through the formulation of the problem how to be intended to model these phenomena mathematically, which does not include all physical and chemical processes in the problem of dispersion of a plume mathematically, but that is understood to be the most relevant and possible as a numerical model that is intended to apply to real problems of environmental engineering. The station consists of two chimneys with a height of 100 m and a diameter of 6 m, with a distance between the chimneys of 20 m,as shown in Fig (2). In order to obtain an accurate result, an area with dimensions of 6,750 × 500 × 1500 m was chosen, as shown in Fig (3).

Figure (1) Nassiriya Thermal Power Station (Iraq, Nassiriya City) [10].

Figure (2) View of the chimneys of Nassiriya Thermal Power Station (Iraq, Nassiriya City) [11].

4. Mathematical model

4.1 Governing equations

The Governing equations of the dispersion model are presented. The fluid mechanics (continuity, momentum, energy, and Navier-Stokes) are generally formed. The equations are, in general, shown below as [12,13]

The continuity equation:

$$\frac{\partial u_j}{\partial x_j} = 0 \qquad (3.1)$$

Momentum equation:

$$\frac{\partial \rho u_i}{\partial t} + \frac{\partial}{\partial x_j}\left(\rho \mathrm{i} u_j\right) = -\frac{\partial p'}{\partial x_i} + \frac{\partial}{\partial x_j}\left[\mu_{eff}\left(\frac{\partial u_i}{\partial x_j} + \frac{\partial u_j}{\partial x_i}\right)\right] - \rho \vec{g} n \qquad (3.2)$$

Here $\mu_{eff} = \mu + \mu_t \quad where\ \mu_t = \rho c_\mu \frac{k^2}{\varepsilon}$

Energy equation:

$$\frac{\partial}{\partial T}\partial(\rho E) + \nabla.\left(\vec{\mathrm{v}}(\rho E + p) = \nabla.\left(k_{eff}\nabla T - \sum \mathrm{j}\ \mathrm{hj}\vec{\mathrm{J}}\mathrm{j} + (\tau eff \cdot \vec{v})\right)\right) +$$

$$Sh \qquad (3.3)$$

4.2 k- ε turbulence model

The k-ε standard model is employed to investigate how turbulence affects flow. Due to its reasonable accuracy, robustness, and economy for a large area of turbulent flows, the standard k-ε model is utilized in heat transfer and industrial flows, which explains its popularity. Launder and Spalding were the ones who first put forth the idea. From the precise transport equation, the transport equation for (k) in this model was derived. Physical considerations were used to arrive at the equation for (ε). Transport the k-ε standard model equations are as follows: [12,13].

The equation for turbulence kinetic energy (k):

$$\frac{\partial k}{\partial t} + \frac{\partial}{\partial x_j}(u_j k) = \frac{\partial}{\partial x_j}\left(\left(\mu + \frac{\mu_t}{\sigma_k}\right)\frac{\partial k}{\partial x_j}\right) + P_k - \rho\varepsilon + P_{kb} \quad (3.4)$$

Turbulent energy dissipation (ε) equation:

$$\frac{\partial \varepsilon}{\partial t} + \frac{\partial}{\partial x_j}(u_j \varepsilon) = \frac{\partial}{\partial x_j}\left[\left(\mu + \frac{\mu_t}{\sigma_\varepsilon}\right)\frac{\partial \varepsilon}{\partial x_j}\right] + \frac{\varepsilon}{k}(C_{\varepsilon 1}P_k - C_{\varepsilon 2}\rho\varepsilon + C_{\varepsilon 1}P_{\varepsilon b}) \quad (3.5)$$

P_k _Turbulence generation due to viscous forces represented as follows:

$$P_k = \mu_t\left(\frac{\partial u_i}{\partial x_j} + \frac{\partial u_j}{\partial x_i}\right)\frac{\partial u_i}{\partial x_j} - \frac{2}{3}\frac{\partial u_k}{\partial x_k}(3\mu_t\frac{\partial u_k}{\partial x_k} + \rho k), \quad (3.6)$$

Where $\sigma_\rho = 0.9, c_\mu = 0.09, C_{\varepsilon 1} = 1.44, C_{\varepsilon 2} = 1.92, \sigma_k = 1, \sigma_\varepsilon = 1.3$

5. Boundary conditions

1. The inlet boundary conditions are as follows:

The inlet boundary conditions are divided into two sections

a. Inlet (velocity inlet):

- Wind speed (2, 4, 6, 8 and 10) m/s and initial gauge pressure (pa) equals zero

- The temperature (T_{wind}=314K)

- Species mass fraction (H_2O= 0.01505, N_2 = 0.75841, O2 = 0.22654).

b. Inlet-chimney 1 and inlet-chimney 2

- Mass flow rate for crude oil (ṁ= 13.47996 and 26.95992) kg/s

- Mass flow rate for natural gas (ṁ= 18.18168 kg/s)

- The wet inlet temperature (T_{in}= 443 K)

- Species mass fractions of crude oil (m) (H_2O = 0.0688, CO_2= 0.159, N_2= 0.698, CO= 0.0402, NO_X= 0.00132, SO_2 =0.02, H_2= 0.0006, O_2= 0.0117)

- Species mass fractions of natural gas (m) (CO=0.104, CO2=0.0769, NO_X =0.00026, SO_2=0, H_2O =0.114,N_2=0.698, H_2=0.00664 and O_2=0)

2. The boundary condition in the outlet

At the exit, the gauge pressure (pa) equals zero

$$\Delta p = 0$$

3. Symmetry:

Symmetry includes the upper and sides.

4. Wall:

The walls are divided into two parts, the chimney wall and the ground wall. No slip boundary condition is imposed.

This boundary conditions were ”wall” for the chimney walls and ground, “velocity inlet” for the wind inlet and chimney opening, “symmetry” for the side walls and top wall, and “pressure outlet” for the outlet, as shown in Fig (3).

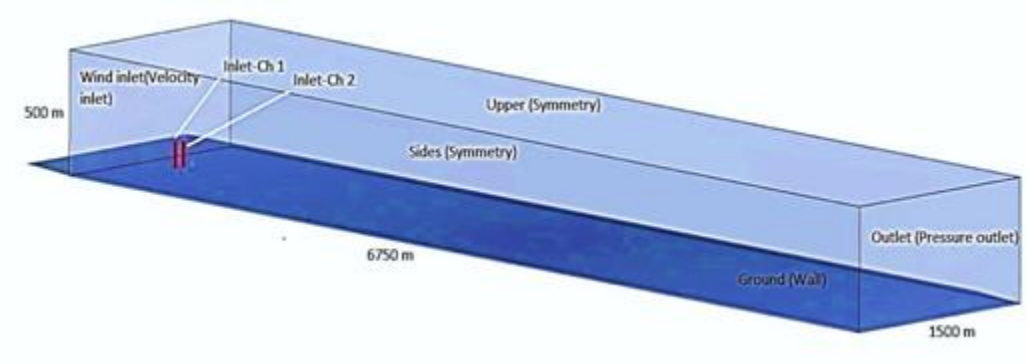

Figure (3) Computational domain and boundary conditions for the Nassiriya TPP simulation.

6. Computational Fluid Dynamics

Many academics throughout the world now rely on computational fluid dynamics (CFD) to anticipate internal and exterior flows. The basic numerical-based techniques were built on a set of computer programs that can be easily programmed on a personal computer (PC). Because of this change in CFD science with computer programs, we have to use evolved codes for numerical analysis on the computer to solve our problems. This chapter contains the numerical analysis of the flow of gases and liquids in the field of this study (modeling the effect of combustion products of the power plant). The code FLUENT simulates turbulent three-dimensional problems (compressible or not), the version ANSYS FLUENT 2020 is a CFD program to simulate the problem with the numerical model in the solution of turbulent flows, which can be formed mathematically by the equations of conservation of mass, the amount of motion and energy. Some test problems are three-dimensional. For these problems, the simulations are performed by changing the considered directions of the program 3D. For example, the problem is simulated by a 3D mesh in the directions (x, y, z).

6.1 The numerical algorithm

The simple algorithm method (Semi - Implicit - Method for Pressure Linked Equations) was introduced in the early 1970s at Imperial College in London by Prof. Brian Spalding and SuhasPatankar and has since been used extensively by many researchers to address various flow and heat transfer issues In computational fluid dynamics, the simple approach is typically employed to address the Navier-Stokes equations for the pressure-velocity coupling problem., where the pressure gradient is unknown. This simple algorithm was used by the FLUENT package program described in this study.

6.2 Meshing

The second step required after the design of the model under study to complete the CFD simulation is the generation of the corresponding mesh. The generation of computer meshes has always been the subject of intense research, as it is typically used for physical simulations such as finite elements or computational fluid dynamics to solve the three-dimensional continuity, momentum, and energy equations. Mesh obstetrics is the process of creating a polyhedral or polygonal mesh that approximates the geometric domain. In this study, ANSYS Workbench 2020 R2 was used for this purpose, It provides a variety of meshes, including hexahedral and tetrahedral

meshes that can be structured or unstructured. Different meshes were used due to the different characteristics of the behavior of the variables in the calculation of the flow and the concentration. In the flow case, the main gradients (u, θ, k, and ε) are located near the ground and in terrain areas (topography). Therefore, the mesh should be refined at these locations. In order to increase the production capacity and reduce the computation time, a grid was clustered near the stacks and along the emission range of the emitted gases. The grids used in this work are hexahedral and are explained in Fig (4).

Table (1) Specification of mesh

Parameter	Description
Nodes	6450705
Elements	6143150
Growth rate	1.2
Max size	30.72m
Type mesh	Hexahedral

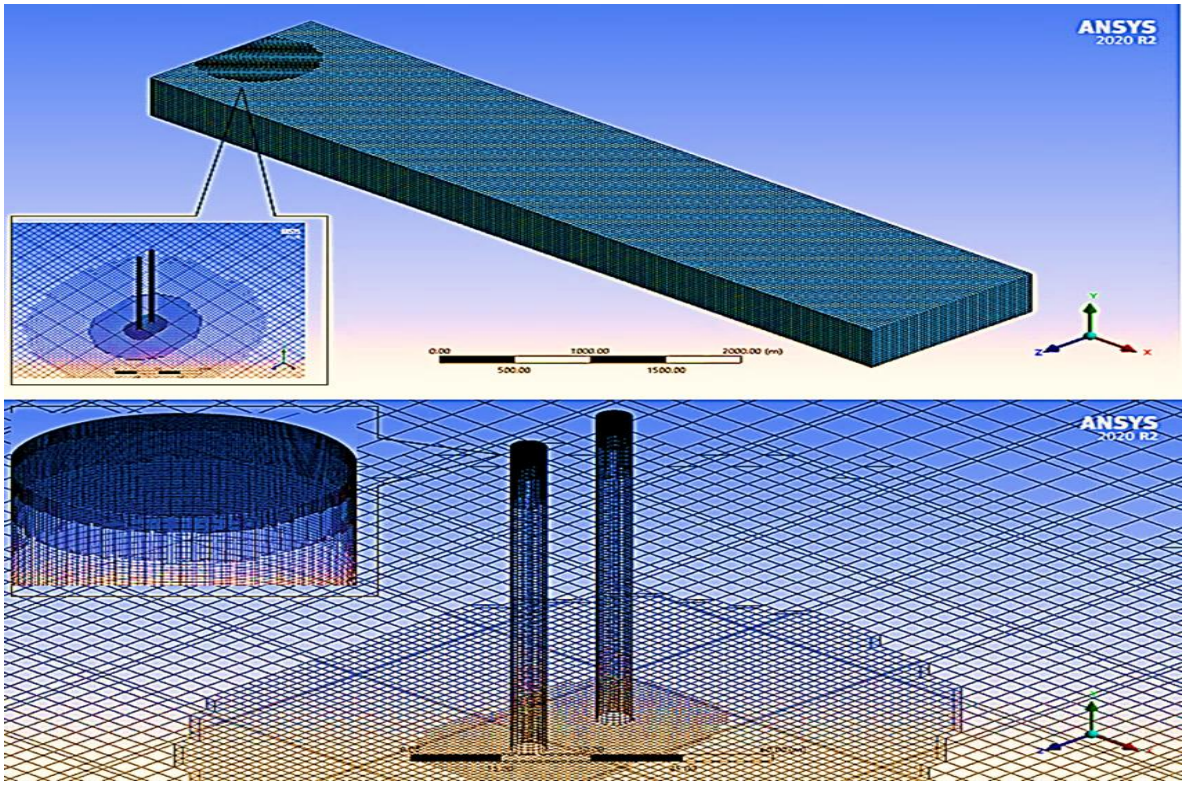

Figure (4) Example of the generation of networks for this work

7. Results and discussion

7.1. Validation

To check the validity, the model is validated with the model that present by Issakhov et al.[14]. Fig (5) shows the vertical concentration profiles at different distances (x/H=5, 10, 15 and 20, where H=300 m) from the pollution sources at the different heights. It can be seen from the figure that there is an acceptable agreement between the results and the average error is about (0.1 - 0.3)%.

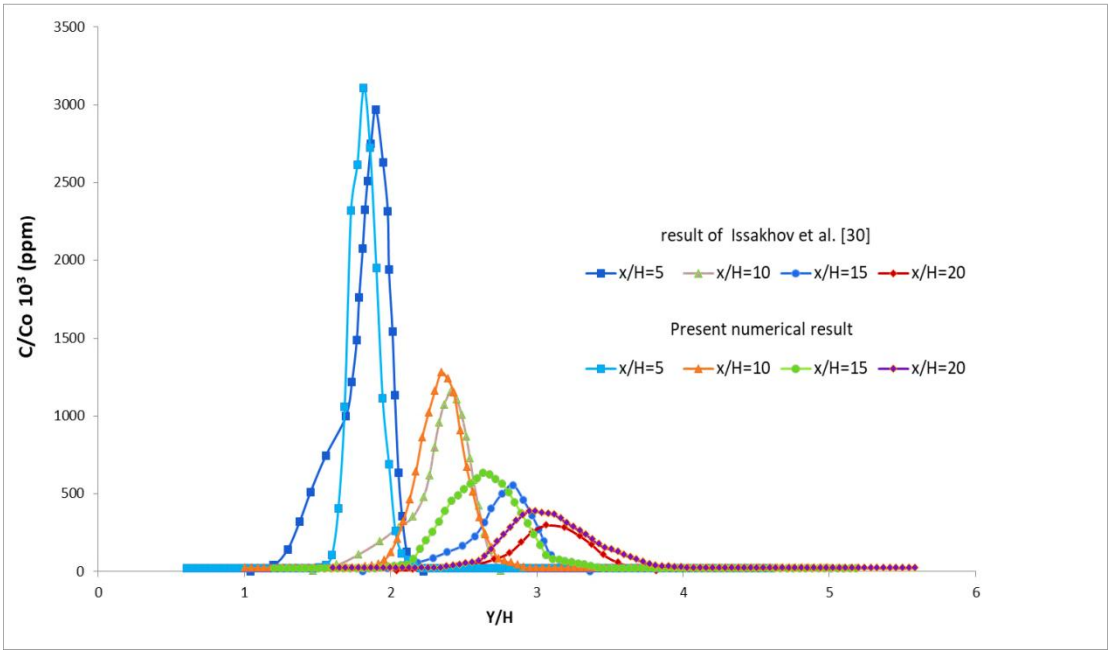

Figure (5) Vertical concentration profiles at variousdistances from the pollution sources at central crosssection (z/H=0).

7.2 Result

Figures (6,7) show the distribution of pollutant con-centration (mass fraction) of carbon monoxide (CO), and carbon dioxide (CO_2) in the case of liquid fuel crude oil for a mass flow of 26.95992 kg/s for each chimney at a wind velocity of (2 m/s) at an angle of 90^o. In the drawing, it is noted that the concentration is distributed over different areas. At the beginning of the smoke exit area from the chimney, the concentration is high, at part (a) of Figures, because the wind speed here is low, so the pollutants descend quickly to the ground surface due to the weight of the pollutants. The second area is the diffusion area, which is the mixing of the pollutant with the air, and the concentration starts to decrease due to dilution and diffusion in parts (b, c) of Figures. The third

region is the vanishing region, where the concentration decreases and approaches zero because the amount of air is greater than the amount of pollutant due to the dispersion velocity in part (d) of Figures.

Figures (8 and 9) present the distribution of pollutant concentration (CO, CO_2) in the state of liquid fuel crude oil at a wind speed (10 m / s) at an angle of 90^o for a mass flow of 26.95992 kg / s per stack. It is noted in the drawing that the concentration is distributed over various areas. At the start of the gas exit area of the chimney, the concentration is high, at part (a) of the figures, because the wind speed is low here, so the pollutants fall quickly to the ground. The second area is the area of diffusion, where the pollutant mixes with the air, and the concentration decreases due to dilution and diffusion, at (b, c) of the figures. The third region is the scattering region, where the concentration decreases and approaches zero because the amount of air is greater than the amount of pollutant due to the speed of dispersion at part (d) of the figures.

The pollutant concentration distribution (CO, CO_2) for gaseous fuel natural gas at a wind velocity of (2m/s) at a 90^o angle and a mass flow rate of 18.18168 kg/s for each chimney depict in Figures (10, 11). The concentration is spread across the drawing in several spots. The concentration is high because the wind speed is low at the beginning of the smoke departure area from the chimney, as shown in Fig (a), and the pollutants descend quickly to the ground surface. The second zone is the diffusion area, which is the mixing of the pollutant with the air, and the concentration begins to diminish owing to dilution and diffusion at parts (c, b) of the figures. The vanishing region is the third region in part (d) of the figures, where the concentration declines and approaches zero since the amount of air is higher than the amount of pollutant due to the dispersion speed.

Figures (12, 13) illustrate the pollutant concentration distribution (CO, CO_2) for gaseous fuel natural gas at a mass flow rate of 18.18168 kg/s for each chimney at a 90^o angle from a wind velocity of 10 m/s. The concentration is dispersed throughout the drawing. Since there is little wind at the beginning of the gas exit area from the chimney, there is a high concentration of pollutants at part (a) of Figure, .where they quickly reach the ground. The concentration begins to decline owing to dilution and diffusion at portions (c, b) of the figures in the second area, which is the area of diffusion or mixing of the pollutant with the air. Due to the dispersion velocity at portion (d) of the figures, the amount of air is more than the amount of pollutant in the vanishing zone, which is the third region where the concentration decreases and approaches zero.

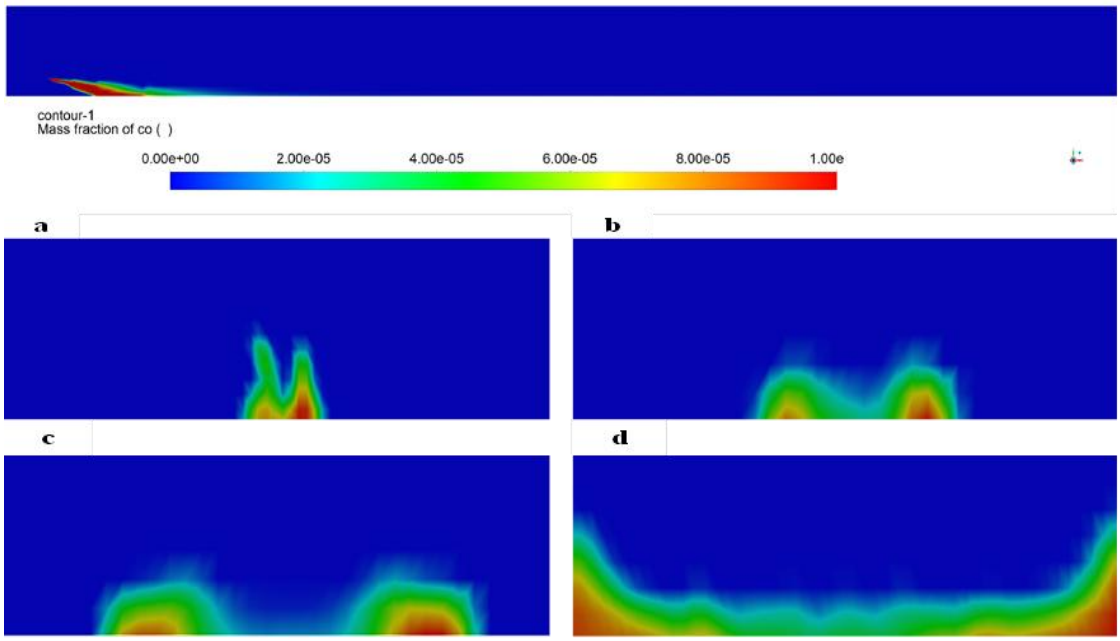

Figure (6) Distribution and comparison of CO mass fraction profiles for crude oil fuel of 26.95992 kg/s for different distances: (a) 406 m, (b) 812 m, (c) 1625 m and (d) 6500 m. at 2 m/s.

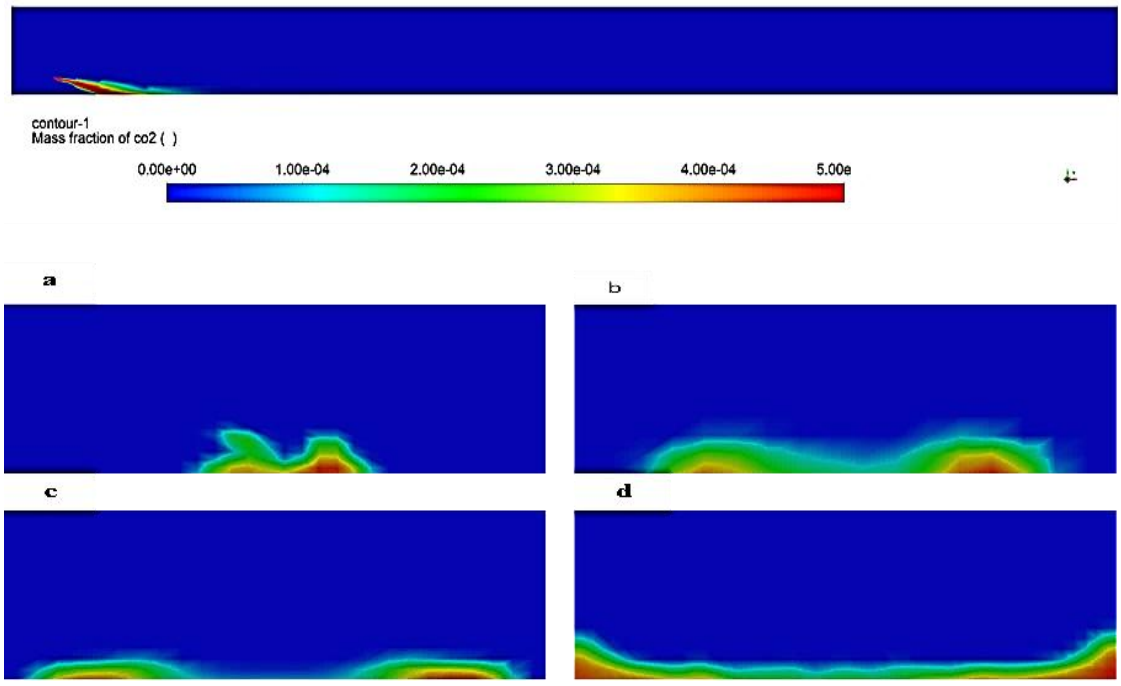

Figure (7) Distribution and comparison of CO_2 mass fraction profiles for crude oil fuel of 26.95992 kg/s for different distances: (a) 406 m, (b) 812 m, (c) 1625 m and (d) 6500 m. at 2 m/s.

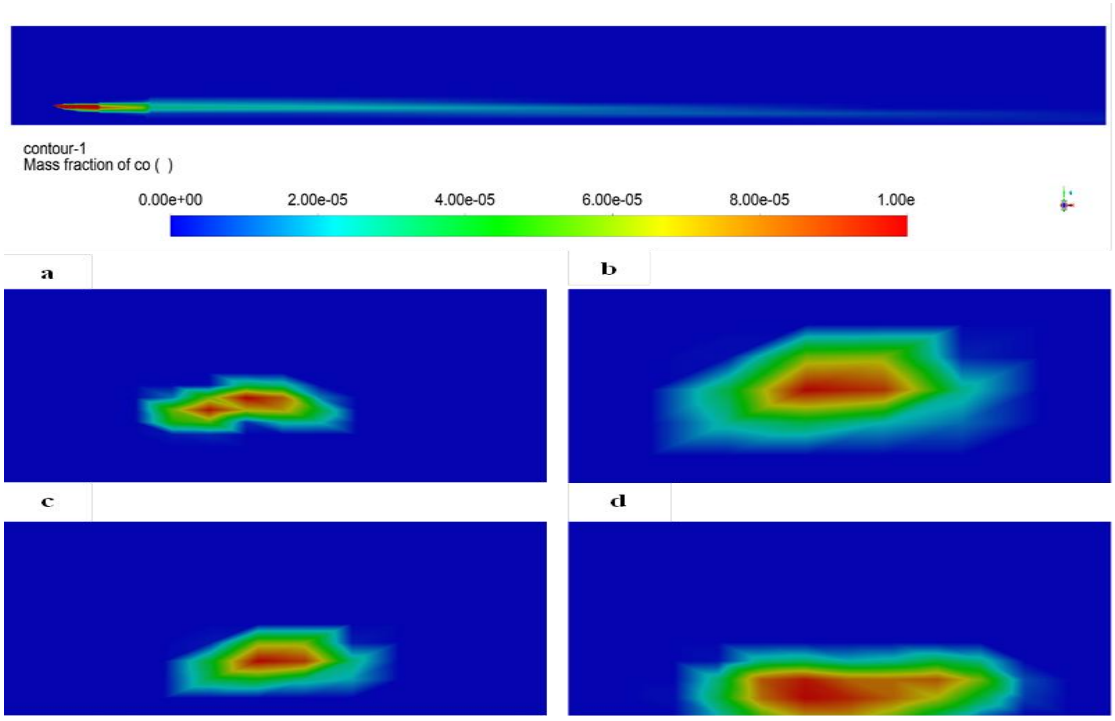

Figure (8) Distribution and Comparison of CO mass fraction profiles for crude oil fuel from 26.95992 kg/s for different distances: (a) 406 m, (b) 812 m, (c) 1625 m and (d) 6500 m. at 10 m/s.

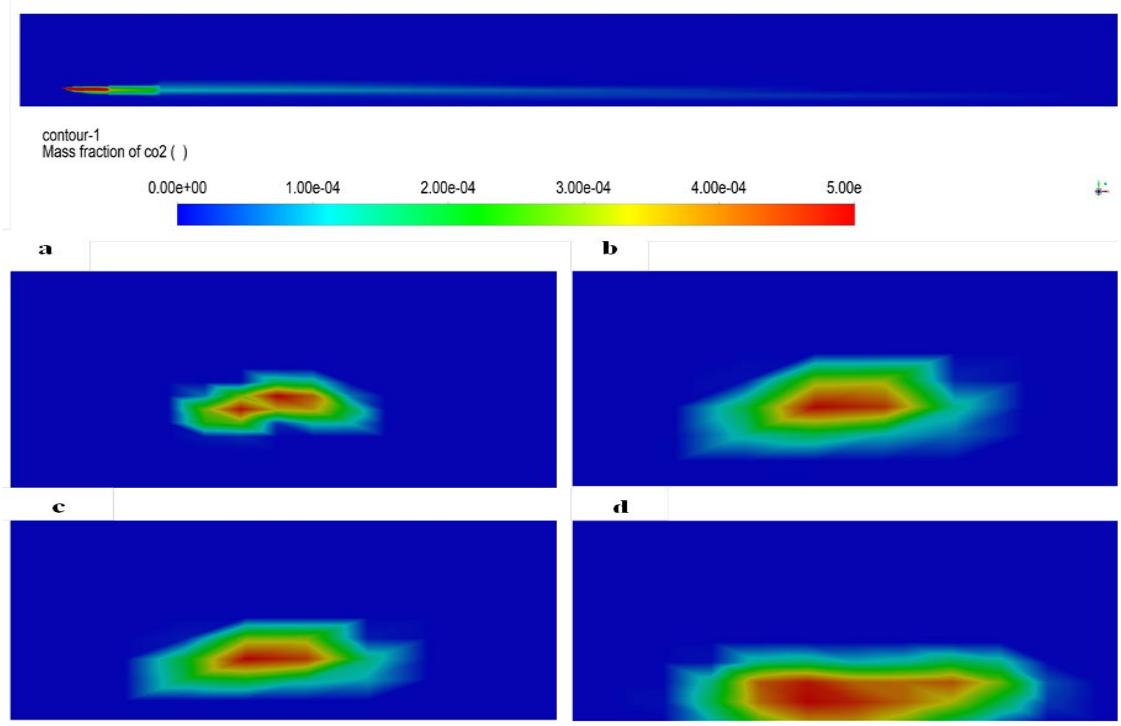

Figure (9) Distribution and comparison of CO_2 mass fraction profiles for crude oil fuel from 26.95992 kg/s for different distances: (a) 406 m, (b) 812 m, (c) 1625 m and (d) 6500 m. at 10 m/s.

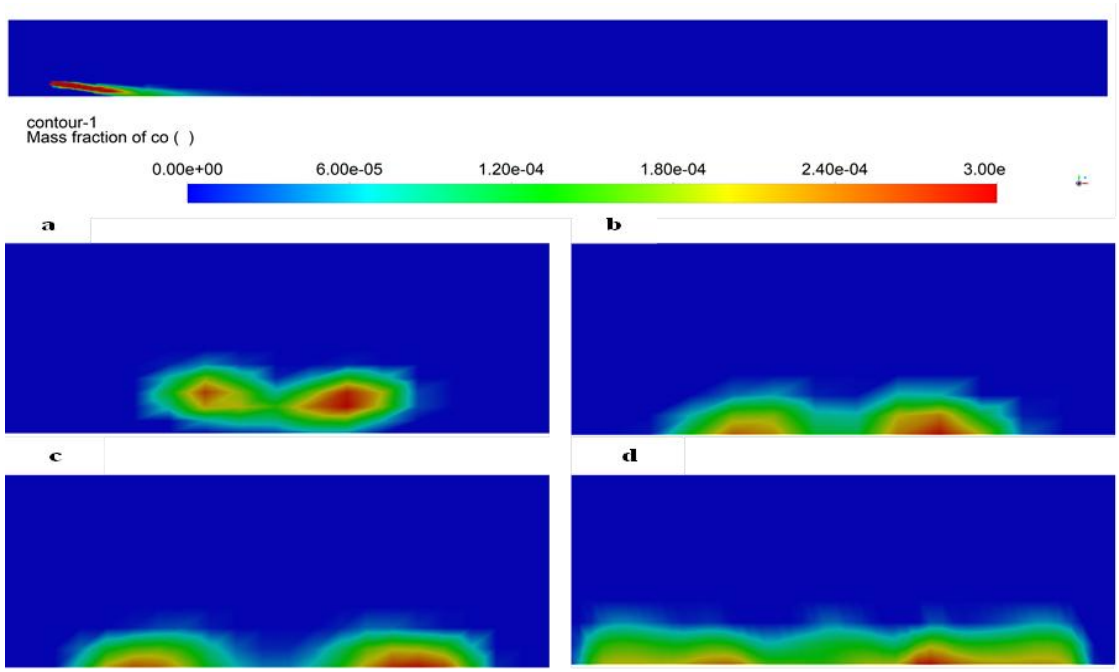

Figure (10) Distribution and comparison of CO mass fraction profiles for natural gas fuel from 18.18168 kg/s kg/s for different distances: (a) 406 m, (b) 812 m, (c) 1625 m and (d) 6500 m. at 10 m/s.

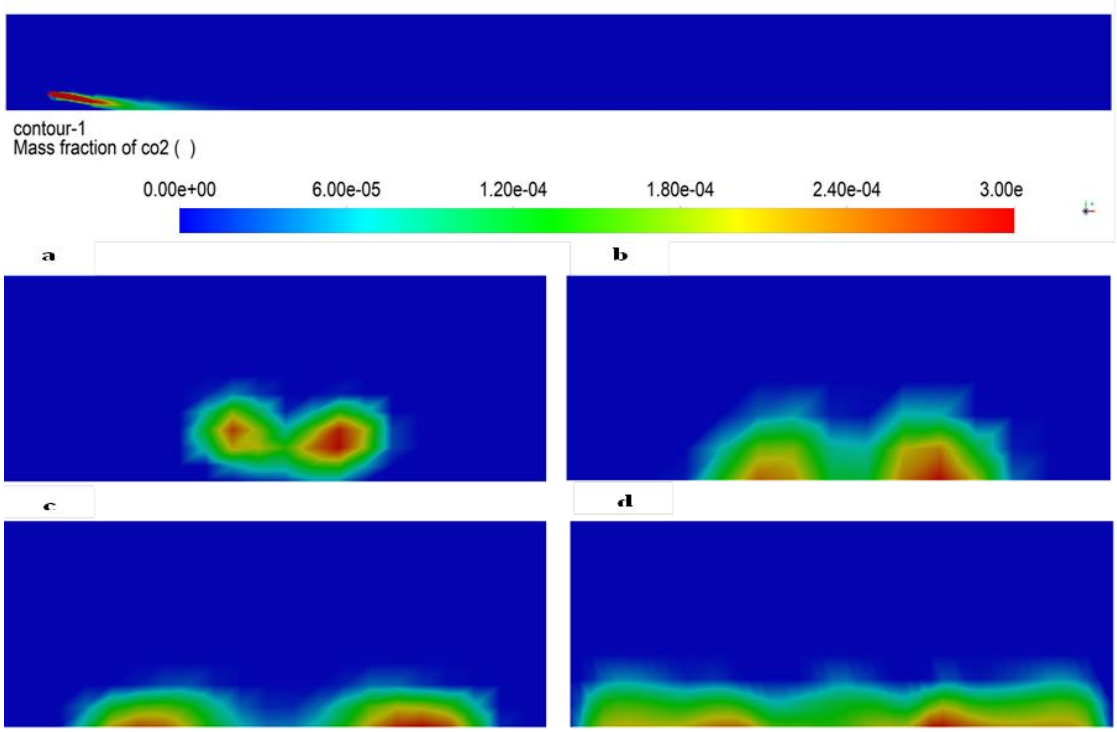

Figure (11) Distribution and comparison of CO_2 mass fraction profiles for natural gas fuel from 18.18168 kg/s kg/s for different distances: (a) 406 m, (b) 812 m, (c) 1625 m and (d) 6500 m. at 2 m/s.

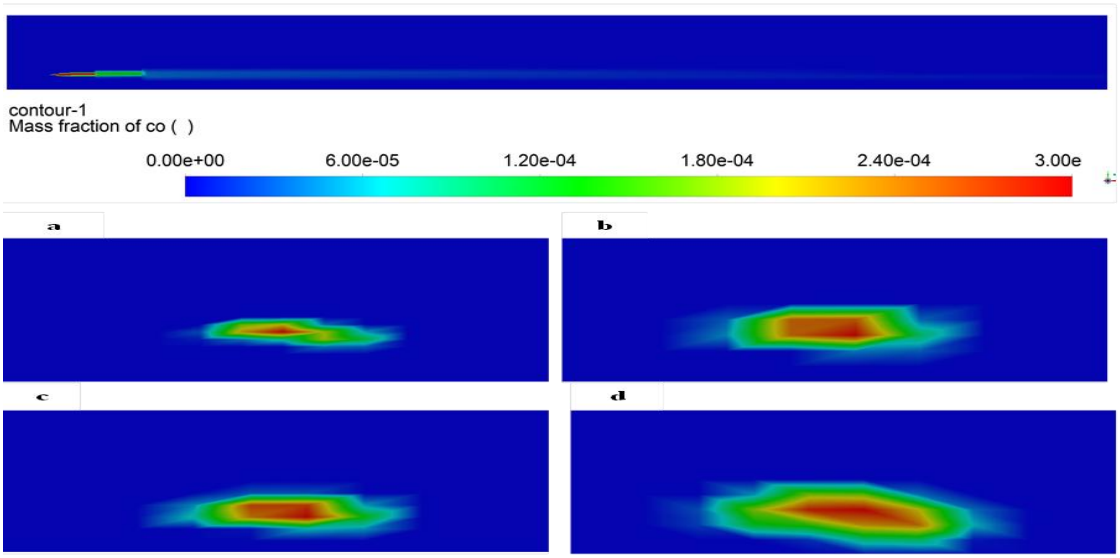

Figure (12) Distribution and comparison of CO mass fraction profiles for natural gas fuel from 18.18168 kg/s kg/s for different distances: (a) 406 m, (b) 812 m, (c) 1625 m and (d) 6500 m. at 10 m/s.

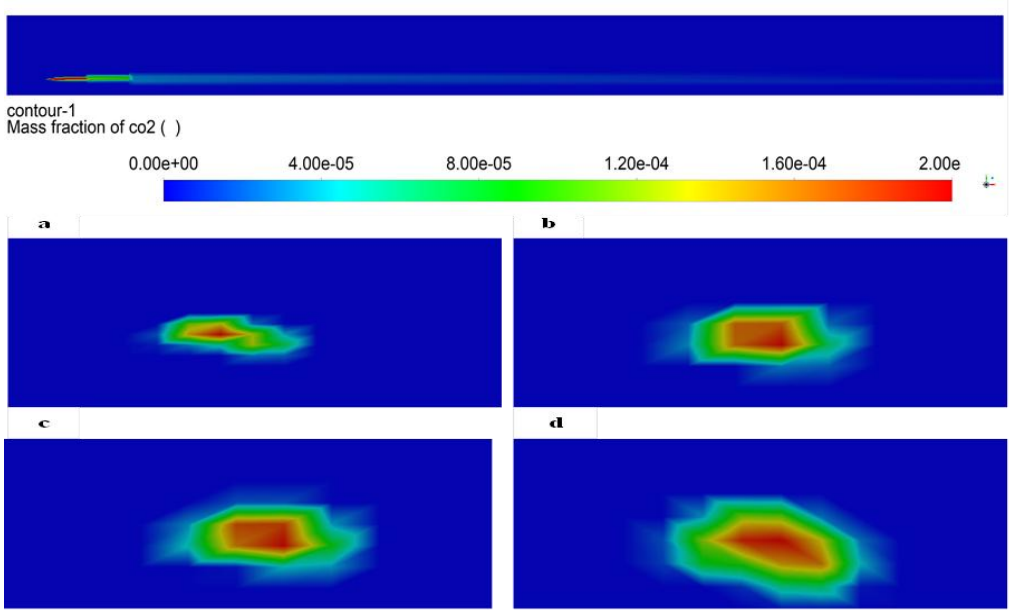

Figure (13) Distribution and comparison of CO_2 mass fraction profiles for natural gas fuel from 18.18168 kg/s kg/s for different distances: (a) 406 m, (b) 812 m, (c) 1625 m and (d) 6500 m. at 10 m/s.

The relationship between the wind speed and the concentration (maximum mass fraction) of (CO, CO_2, SO_2, and NO_x) for a mass flow of 26.95992 kg/s for each stack, fuel type crude oil, and a directional angle of 90o are illustrated in Figures (14, 15, 16, 17). Results showed that at a distance

of 203 m, the concentration is inversely proportional to the wind speed. At a distance of 406 m and a wind velocity of (2-4)m/s, the concentration is directly proportional to wind speed, and from (4m/s-10m/s), the concentration is inversely proportional to wind speed, and at a distance of (812-6500)m, the wind speed is approximately stable above the pollutant concentration, This means that as the distance increases, the concentration decreases due to the phenomenon of diffusion. As the speed increases, the concentration decreases until it disappears due to the diffusion speed and the dilution rate, and the maximum CO concentration for a wind velocity of (2 m/s) is (0. 000594) at a distance of 203 m. The maximum CO concentration at a wind velocity of (10 m/s) is (0.000409) at a distance of 203 m.

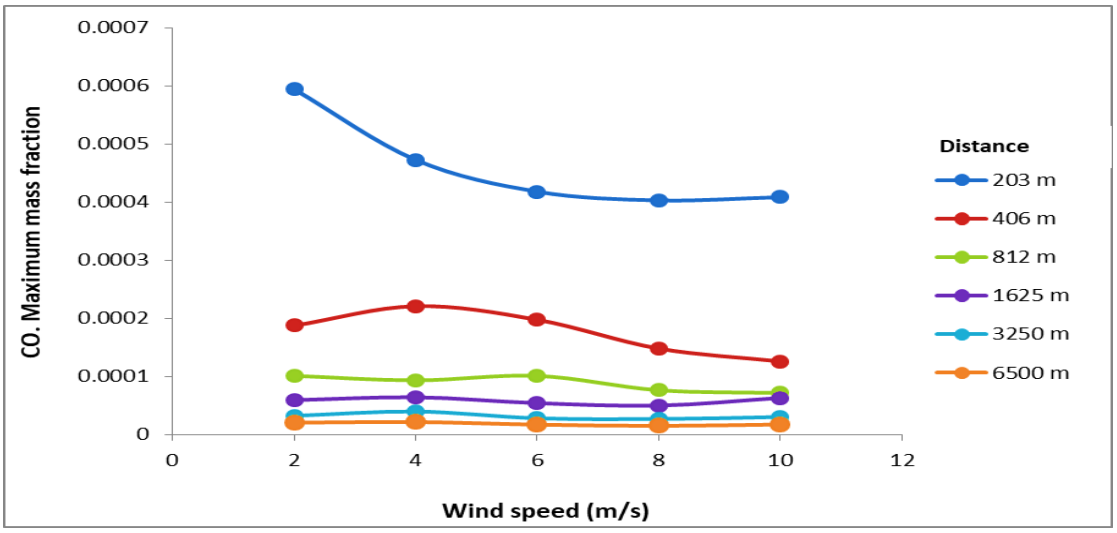

Figure (14) Profiles of CO mass fraction at different at different distances.

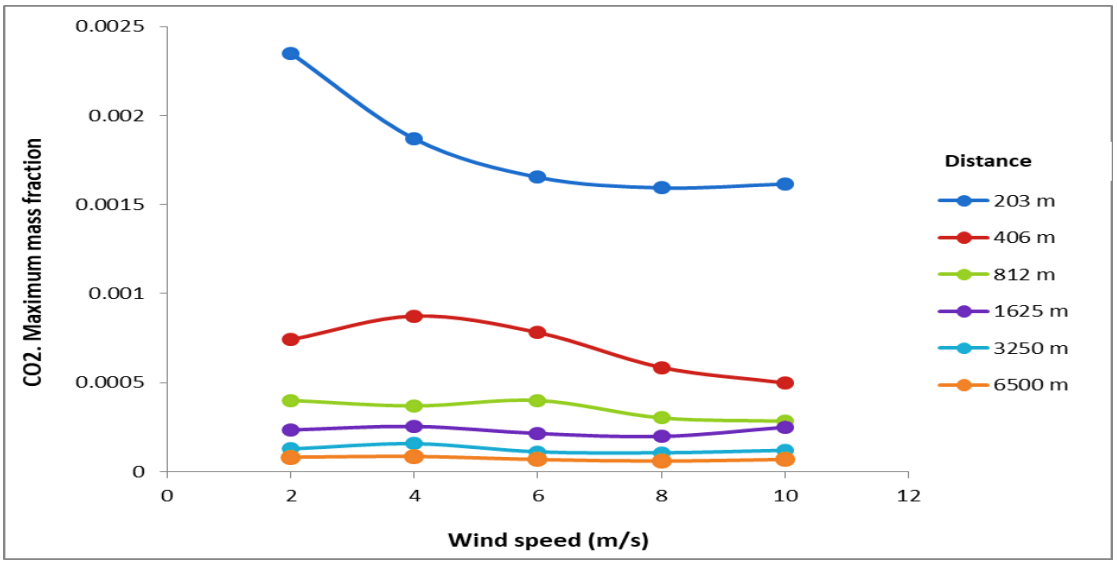

Figure (15) Profiles of CO_2 mass fraction at different at different distances.

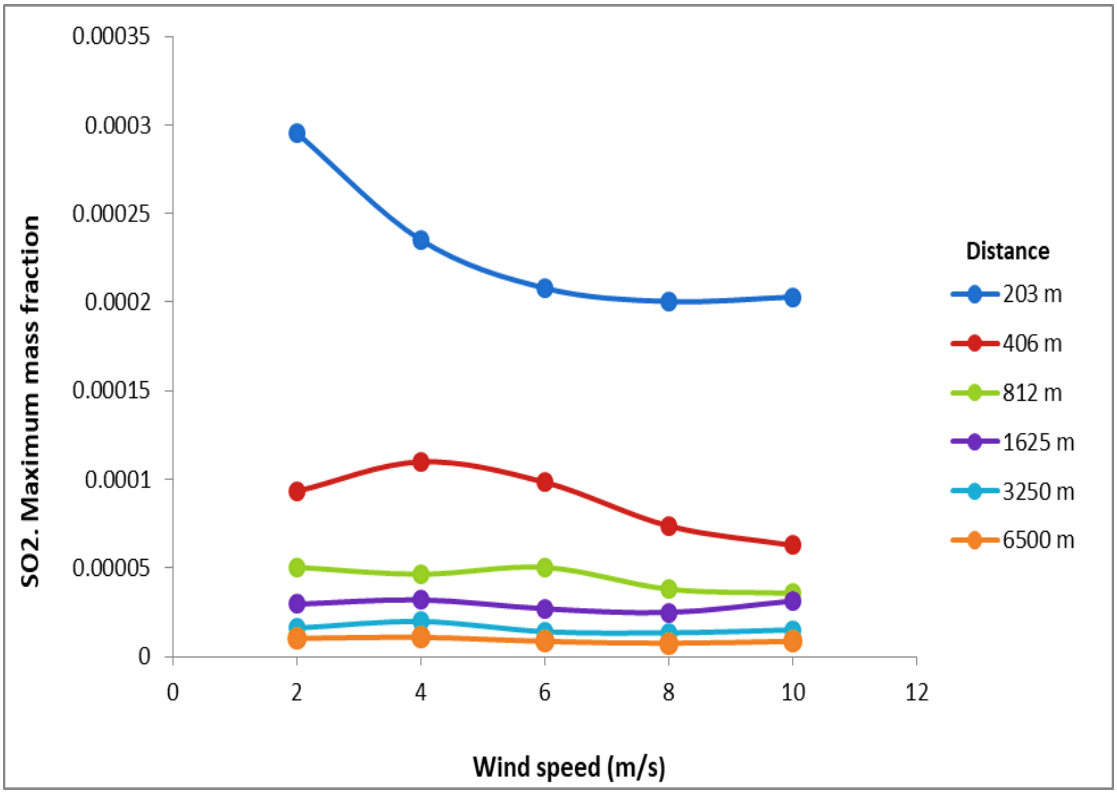

Figure (16) Profiles of SO_2 mass fraction at different at different distances.

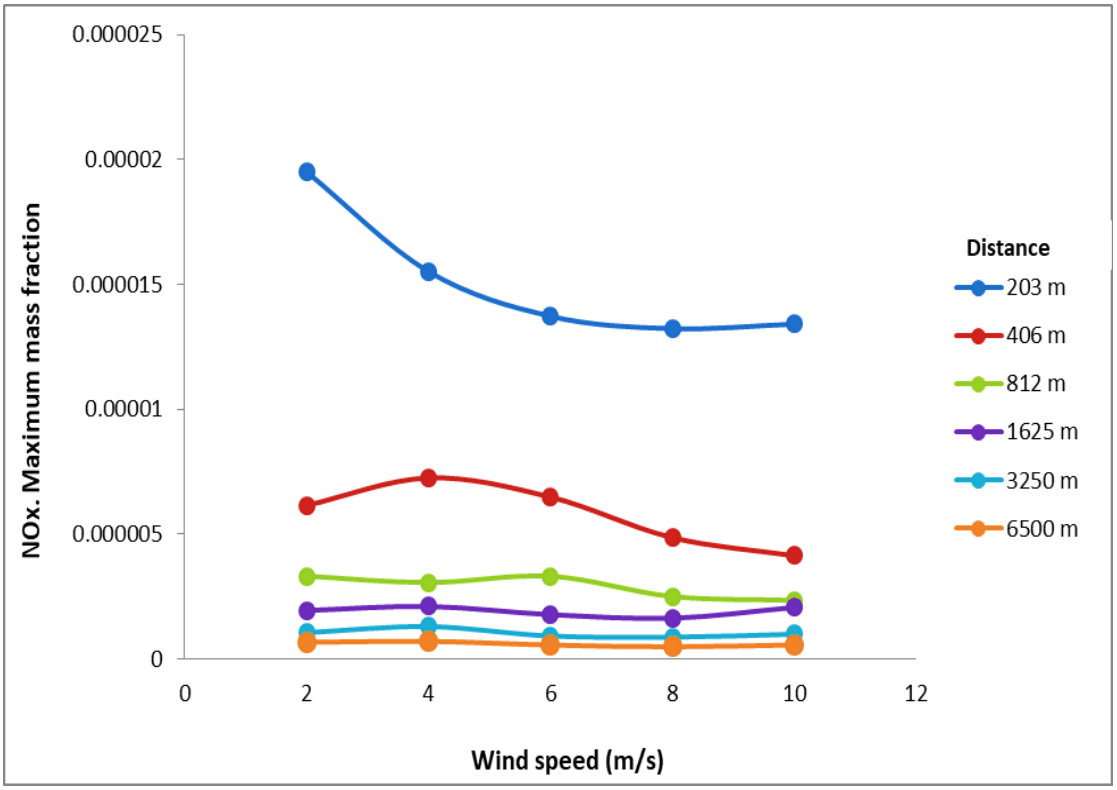

Figure (17) Profiles of NOx mass fraction at different at different distances.

Figure (18) presents the relationship between the fuel type and the concentration (maximum mass fraction) of carbon dioxide (CO) for a mass flow rate of crude oil of 26.95992 kg/s and a mass flow rate of natural gas of 18.18168 kg/s for each chimney at a wind velocity of 2 m/s and a direction angle of 90°. It is found that the concentration of gaseous fuel (natural gas) for each distance is higher than that of liquid fuel crude oil because the air is not enough, the combustion becomes incomplete, and depending on the operating speed of the station, it is recommended to increase the amount of air in this case to achieve complete combustion. The maximum CO concentration for natural gas fuel type is (0.000971) at a distance of 203 m. The lowest (CO) concentration for the fuel type crude oil is (0.0000207) at a distance of 6500 m.

The relationship between the fuel type and the concentration (maximum mass fraction) of carbon dioxide (CO_2) and nitrogen oxides (NO_x) for a mass flow of crude oil of 26.95992 kg/s and a mass flow of natural gas of 18.18168 kg/s for each chimney, at a wind speed of 2 m/s and a directional angle of 90° is shown in Figures (19, 20). Results indicate that the concentration of liquid fuel (crude oil) is higher than that of gaseous fuel (natural gas), and the maximum CO_2 concentration for the type of fuel (crude oil) is (0.00235) at a distance of 203 m. The minimum (CO_2) concentration for a fuel type (natural gas) is (0.0000362) at a distance of 6500 m.

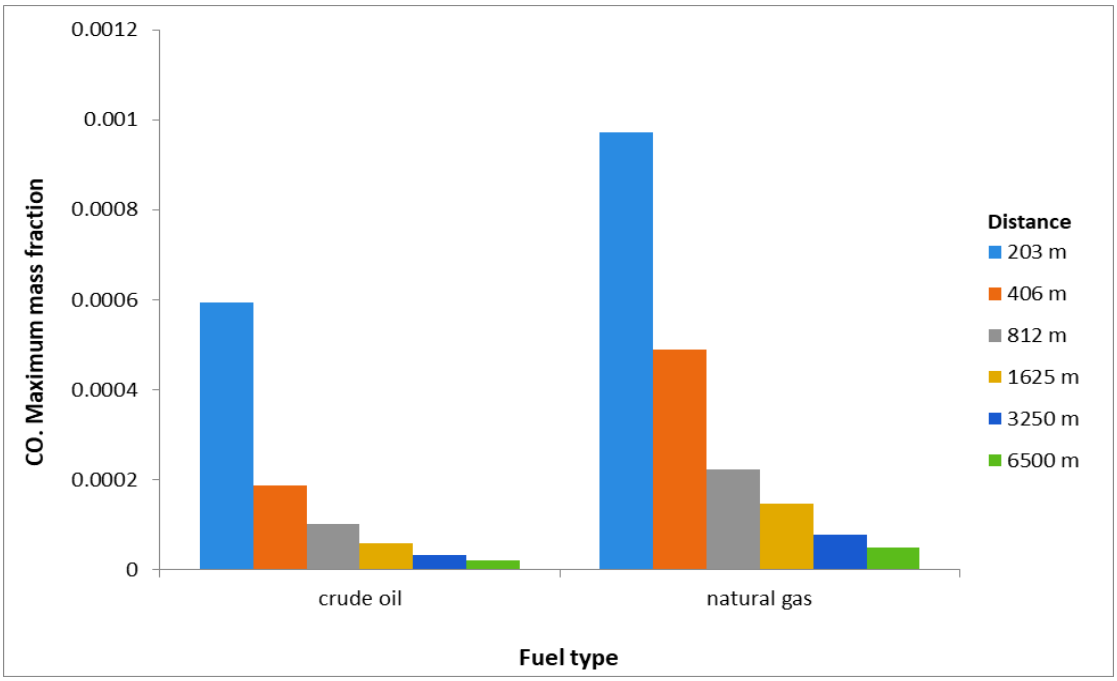

Figure (18) Comparison of CO mass fraction profiles for crude oil and natural gas fuel from at different distances, at 2 m/s.

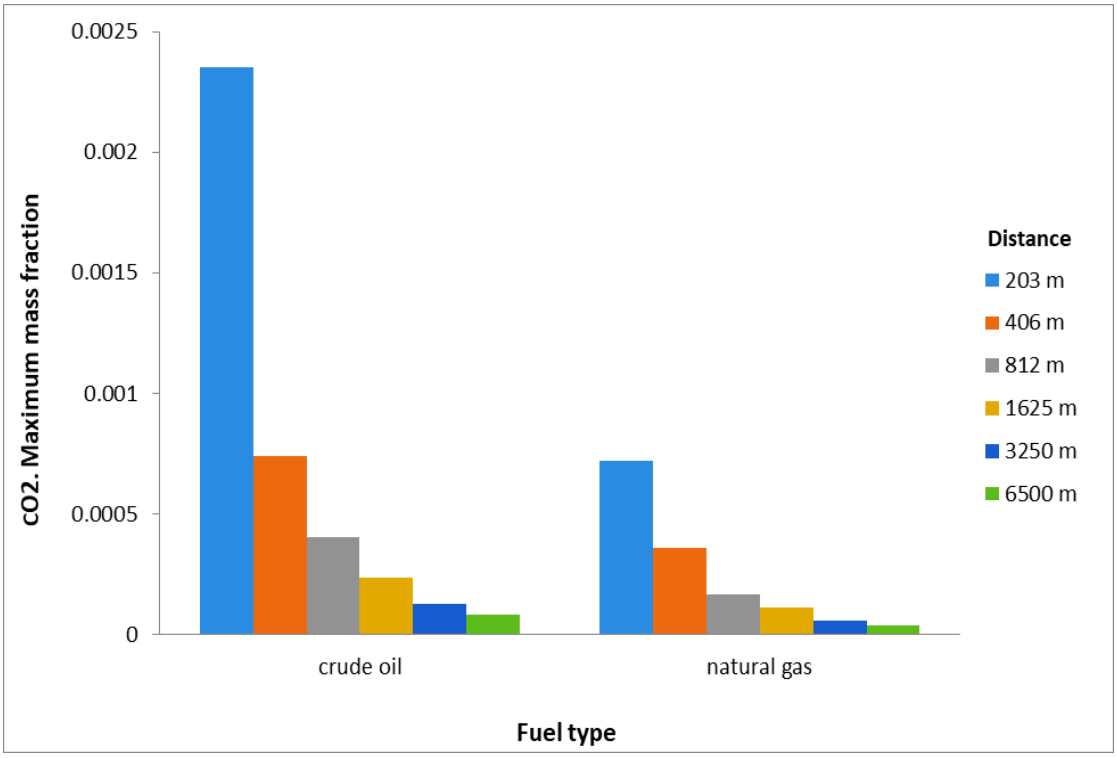

Figure (19) Comparison of CO_2 mass fraction profiles for crude oil and natural gas fuel from at different distances, at 2 m/s.

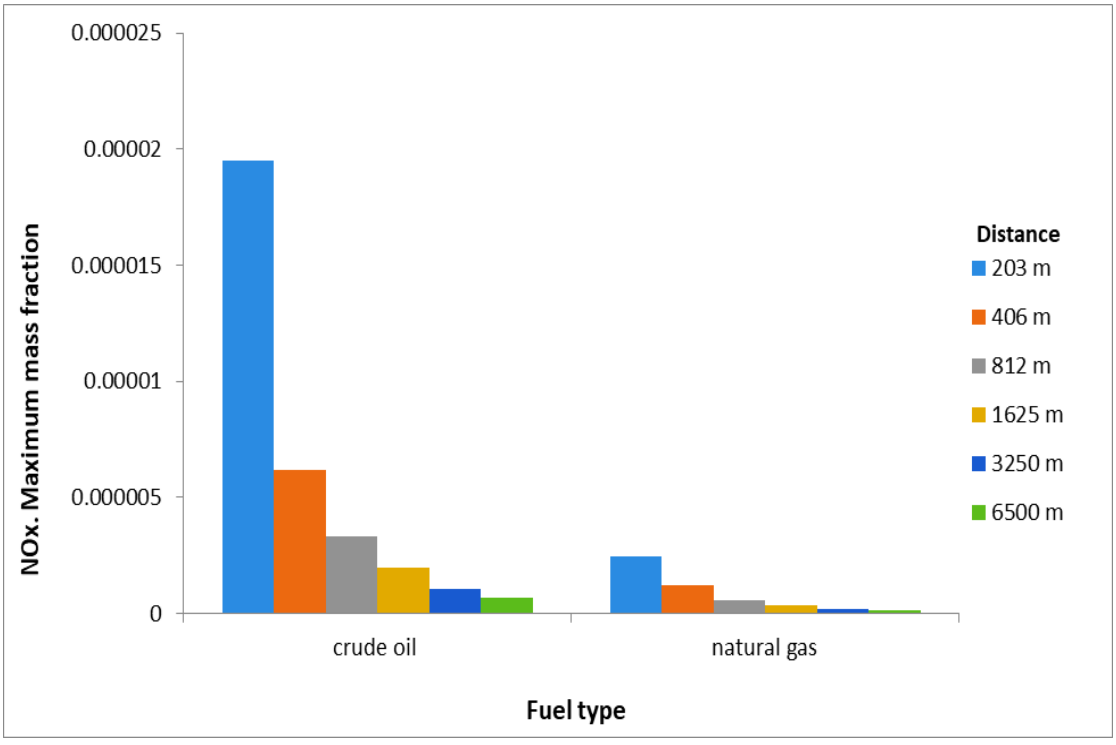

Figure (20) Comparison of NOx mass fraction profiles for crude oil and natural gas fuel from at different distances, at 2 m/s.

8. Conclusions

The numerical model was designed, simulated, and tested for the modeling of pollutant dispersion from the stacks of thermal power plants. From the simulation results presented, the framework allows to draw the following conclusions:

1. The height of the chimney reduces the concentration of pollution, which has a bad effect on life on earth since most of the plumes go a long distance and the percentage of concentration becomes very low.

2. The high smoke velocity of the chimney gives the smoke plumes a great height and distance to reduce the concentration because the high velocity should give a good dispersion of the smoke plumes.

3. The best smoke velocity is more than 1.5 of the air velocity because the high air velocity causes a downdraft for the pollutants, and the very low velocity is not able to remove the smoke plumes over long distances.

4. Pollutants are spread over a large area when the height of the chimney is high. Also, when the wind speed is high, pollution will spread far from its source, and when the wind speed is low, the highest concentration of pollution is at ground level.

5. The concentration of pollutants in liquid fuels (crude oil) is higher than the concentration of pollutants in gaseous fuels (natural gas), where the maximum concentration of carbon dioxide (CO2) in liquid and gaseous fuels is (0.0000362, 0.00235, respectively) of a wind velocity of 2 m/s and a distance of 203 m.

6.The relationship between distance and concentration is an inverse relationship at different wind speeds, which means that concentration decreases with increasing distance due to the diffusion phenomenon. With increasing speed, the concentration decreases due to the diffusion speed and dilution rate. The maximum concentration of carbon dioxide at wind velocities of 2 and 10 m/s is 0.000594 and 0.000409, respectively.

References

[1] Asif, M., & Muneer, T. (2007). Energy supply, its demand and security issues for developed and emerging economies. Renewable and sustainable energy reviews, 11(7), 1388-1413.

[2] Hannun, R. M. (2009). Three Dimensional Aerodynamic and Temperature Predictions for Nassiriya Power Plant Boiler Furnace (Doctoral dissertation, Ph. D. Thesis, College of Engineering, Basrah University, Iraq).

[3] Schneider, D. R., & Bogdan, Ž. (2007). Effect of heavy fuel oil/natural gas co-combustion on pollutant generation in retrofitted power plant. Applied thermal engineering, 27(11-12), 1944-1950.

[4] Alaa H. M. (2009). A theoretical study of pollutant emissions from industrial chimneys. Basra University Library for Department of Mechanical Engineering.

[5] Hannun, R. M., Najim, S. E., Rishack, Q. A., & Syred, N. (2013). Modeling of Pollutants Prediction from Fuel Burning in Oil and Gas Refineries. Engineering and Technology Journal, 31(18 Part (A) Engineering).2014 .

[6] Idrissi, M. S., Ben Salah, N., & Chrigui, M. (2019). Numerical modelling of air pollutant dispersion in complex urban areas: investigation of city parts from downtowns Hanover and Frankfurt. Fluids, 4(3), 137.

[7] Issakhov, A., Alimbek, A., & Issakhov, A. (2020). A numerical study for the assessment of air pollutant dispersion with chemical reactions from a thermal power plant. Engineering Applications of Computational Fluid Mechanics, 14(1), 1035-1061.

[8] El-Fadel, M. (2006). Rapid risk assessment of atmospheric dispersion of stack emissions from Al-Hartha power plant in Iraq Word Bank, environmental assessment (Vol. 2), E1506.

[9] Murtadah, I., Al-Sharify, Z. T., & Hasan, M. B. (2020, June). Atmospheric concentration saturated and aromatic hydrocarbons around Dura refinery. In IOP Conference Series: Materials Science and Engineering (Vol. 870, No. 1, p. 012033). IOP Publishing.

[10] https://iefoundation.net/archives/1002?cat=12

[11] https://www.sahafahh.com/show11613681. html

[12] Issakhov, A., & Mashenkova, A. (2019). Numerical study for the assessment of pollutant dispersion from a thermal power plant under the different temperature regimes. International Journal of Environmental Science and Technology, 16(10), 6089-6112.

[13] Issakhov, A. A., & Baitureyeva, A. R. (2019). Modeling of a passive scalar transport from thermal power plants to atmospheric boundary layer. International Journal of Environmental Science and Technology, 16(8), 4375-4392.

[14] Issakhov, A., Yang, T., & Baitureyeva, A. (2019). CFD simulation of pollution dispersion from thermal power plants in the atmosphere. International Journal of Mathematics and Physics, 10(1), 56-65.